

Weierstraß-Institut
für Angewandte Analysis und Stochastik
Leibniz-Institut im Forschungsverbund Berlin e. V.

Preprint

ISSN 2198-5855

Optimal design of the tweezer control for chimera states

Iryna Omelchenko¹, Oleh E. Omel'chenko², Anna Zakharova¹, Eckehard Schöll¹

submitted: November 28, 2017

¹ Institut für Physik
Technische Universität Berlin
Hardenbergstraße 36
10623 Berlin
Germany
E-Mail: iryna.omelchenko@tu-berlin.de
anna.zakharova@tu-berlin.de
schoell@physik.tu-berlin.de

² Weierstrass Institute
Mohrenstr. 39
10117 Berlin
Germany
E-Mail: oleh.omelchenko@wias-berlin.de

No. 2449
Berlin 2017



2010 *Mathematics Subject Classification.* 34H10, 34C15.

2008 *Physics and Astronomy Classification Scheme.* 05.45.Xt, 05.45.Ra, 89.75.-k.

Key words and phrases. Nonlinear systems, dynamical networks, spatial chaos, chimera state, feedback control.

This work was supported by Deutsche Forschungsgemeinschaft in the framework of Collaborative Research Center SFB 910.

Edited by
Weierstraß-Institut für Angewandte Analysis und Stochastik (WIAS)
Leibniz-Institut im Forschungsverbund Berlin e. V.
Mohrenstraße 39
10117 Berlin
Germany

Fax: +49 30 20372-303
E-Mail: preprint@wias-berlin.de
World Wide Web: <http://www.wias-berlin.de/>

Optimal design of the tweezer control for chimera states

Iryna Omelchenko, Oleh E. Omel'chenko, Anna Zakharova, Eckehard Schöll

Abstract

Chimera states are complex spatio-temporal patterns, which consist of coexisting domains of spatially coherent and incoherent dynamics in systems of coupled oscillators. In small networks, chimera states usually exhibit short lifetimes and erratic drifting of the spatial position of the incoherent domain. A tweezer feedback control scheme can stabilize and fix the position of chimera states. We analyse the action of the tweezer control in small nonlocally coupled networks of Van der Pol and FitzHugh-Nagumo oscillators, and determine the ranges of optimal control parameters. We demonstrate that the tweezer control scheme allows for stabilization of chimera states with different shapes, and can be used as an instrument for controlling the coherent domains size, as well as the maximum average frequency difference of the oscillators.

1 Introduction

Systems of coupled oscillators are a widely studied topic in the area of nonlinear science, they have numerous applications in physics, chemistry, biology, and technology. Synchronization and partial synchronization of oscillators has been in the focus of the studies, including the phenomenon of *chimera states* which are characterized by a hybrid nature of coexisting spatially coherent and incoherent domains [1, 2, 3, 4, 5, 6, 7]. Theoretical studies of chimera states have considered a wide range of large-size networks [8, 9, 10, 11, 12, 13, 14, 15, 16, 17, 18, 19, 20, 21, 22, 23, 24, 25, 26, 27, 28, 29, 30, 31, 32, 33, 34, 35], with a variety of regular and irregular coupling topologies. In experiments, chimera states were first demonstrated in optical [36] and chemical [37, 38] systems, followed by experiments in mechanical [39], electronic [40, 41, 42] and electrochemical [43, 44] oscillator systems as well as Boolean networks [45]. In the framework of phase oscillator systems, analytical insights and bifurcation analysis of chimera states have been obtained in the continuum limit case, which explains the behaviour of very large ensembles of coupled oscillators [46, 47, 48, 49]. Chimera states in small-size networks have attracted attention only recently [50, 51, 52, 53], whereas lab experiments with such networks are usually more realistic. For identification of chimera states, the concept of 'weak chimeras' [50] was introduced, using partial frequency synchronization as the main indicator of such states.

In small-size systems of nonlocally coupled oscillators, chimera states usually have a finite lifetime, and it is known that chimera states are chaotic transients, which eventually collapse to the uniformly synchronized state [14]. Their mean lifetime decreases rapidly with decreasing system size. Moreover, chimera states exhibit a motion of the position of the incoherent domain along the oscillator array. This drift has the statistical properties of a Brownian motion and its diffusion coefficient is inversely proportional to some power of the system size [54].

In phase oscillator systems with more complex coupling functions including higher harmonics or quadratic components [55, 56], chimera states can be stabilized without any external influence. In large networks with nonlocal coupling functions, the drift of chimera states is weak, and collapse is

impossible to observe numerically due to their very long lifetimes. However, in small networks both problems dominate. A control techniques, which allow to overcome these difficulties in phase oscillator networks, have been suggested recently. The lifetime of chimera states as well as their basin of attraction can be effectively controlled by a special type of proportional control relying on the measurement of the global order parameter [57]. The spatial position of the coherent domain of the chimera states can be stabilized by a feedback loop inducing a state-dependent asymmetry of the coupling topology [58], based on the evaluation of a finite difference derivative for some local mean field.

Recently, we proposed a tweezer control scheme for stabilization of chimera states [59], shown schematically in Fig. 1. This control scheme consists of two parts, symmetric and asymmetric, and effectively stabilizes chimera states in small networks of oscillators exhibiting both phase and amplitude dynamics.

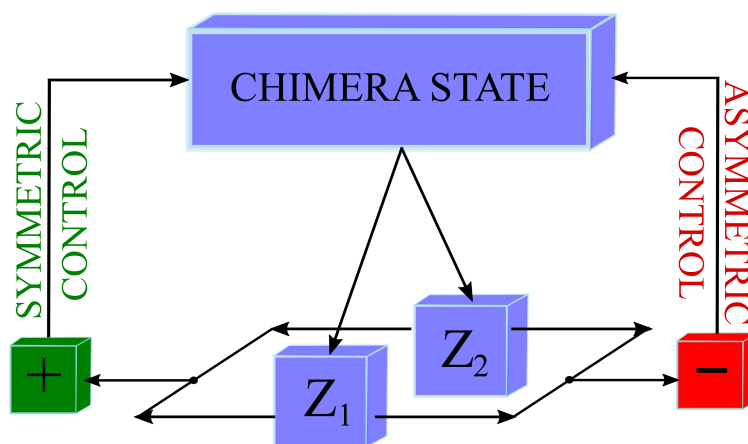


Figure 1: Schematic representation of the tweezer control. Z_1 and Z_2 denote the complex order parameters for one half of the oscillator population, respectively.

In the case of networks of coupled phase and amplitude dynamics, in contrast to pure phase oscillators, a simple analytical study for the continuum limit ($N \rightarrow \infty$) is not possible, therefore we concentrate mainly on the numerical stability analysis. We provide an extensive numerical scan of the oscillators frequency variations in the parameter space, and uncover parameter ranges of symmetric and asymmetric control gains where chimera states are the most pronounced in the sense of frequency differences between oscillators from coherent and incoherent domains and size of the coherent domains. We aim to analyze the influence of the control gain on the shape of the stabilized chimera states, and detect parameter regimes where tweezer control is the most effective. This can be useful in the experiments in order to choose the control gains appropriately for the *optimal* control of chimera states. Additionally, we analyze the influence of the individual oscillator dynamics on the controlled system for networks of Van der Pol and FitzHugh-Nagumo oscillators, and demonstrate that optimal tweezer control allows for stabilization of variable chimera patterns with different sizes of coherent domains. Moreover, in networks of FitzHugh-Nagumo oscillators, the control enables the stabilization of chimera states with multiple incoherent domains even in small networks.

2 Tweezer control in networks of Van der Pol oscillators

We consider a system of N identical nonlocally coupled Van der Pol oscillators $x_k \in \mathbb{R}$ given by

$$\begin{aligned} \ddot{x}_k &= (\varepsilon - x_k^2)\dot{x}_k - x_k \\ &+ \frac{1}{R} \sum_{j=1}^R [a_-(x_{k-j} - x_k) + b_-(\dot{x}_{k-j} - \dot{x}_k)] \\ &+ \frac{1}{R} \sum_{j=1}^R [a_+(x_{k+j} - x_k) + b_+(\dot{x}_{k+j} - \dot{x}_k)]. \end{aligned} \quad (1)$$

Here, the scalar parameter $\varepsilon > 0$ determines the internal dynamics of all individual elements. For small ε the oscillation of a single element is sinusoidal, while for large ε it is a strongly nonlinear relaxation oscillation. Each element is coupled with R nearest neighbours to the left and to the right. We assume that the oscillators are arranged on a ring (i.e., periodic boundary conditions) such that all indices in Eq. (1) are modulo N . The coupling constants in position and velocity to the left and to the right are denoted as a_- , a_+ and b_- , b_+ , respectively.

For the sake of simplicity we assume

$$a_- = a_+ = a, \quad b_- = a\sigma_-, \quad b_+ = a\sigma_+, \quad (2)$$

with rescaled coupling parameters a , σ_- and σ_+ .

We define two complex order parameters

$$Z_1(t) = \frac{1}{[N/2]} \sum_{k=1}^{[N/2]} e^{i\phi_k(t)} \quad (3)$$

$$Z_2(t) = \frac{1}{[N/2]} \sum_{k=1}^{[N/2]} e^{i\phi_{N-k+1}(t)}, \quad (4)$$

where $\phi_k(t)$ is the geometric phase of the k -th oscillator computed from

$$e^{i\phi_k(t)} = (x_k^2(t) + \dot{x}_k^2(t))^{-1/2} (x_k(t) + i\dot{x}_k(t)). \quad (5)$$

As in our previous work, the tweezer feedback control [59] is defined in the form

$$\sigma_{\pm} = K_s \left(1 - \frac{1}{2}|Z_1 + Z_2| \right) \pm K_a (|Z_1| - |Z_2|). \quad (6)$$

The control term has two parts referred to as symmetric and asymmetric controls, see Fig. 1. The symmetric control is analogous to the proportional control suggested for phase oscillators in [57]. It is defined as a feedback loop between coupling parameters σ_{\pm} and the global Kuramoto order parameter

$$|Z_s| = \frac{|Z_1 + Z_2|}{2}.$$

The aim of this feedback loop is to suppress the collapse of small-size chimera states. The asymmetric control is defined as another feedback loop between coupling parameters σ_{\pm} and the difference

$$Z_a = |Z_1| - |Z_2|.$$

This difference indicates a relative shift of the chimera's incoherent domain with respect to the center of the oscillator array $1, \dots, N$. If the incoherent domain of the chimera state moves towards larger indices ($|Z_1| > |Z_2|$), the difference is positive, and $\sigma_+ > \sigma_-$. In the opposite case, when the incoherent domain is shifted towards smaller indices ($|Z_1| < |Z_2|$), we obtain $\sigma_+ < \sigma_-$. An imbalance between σ_+ and σ_- introduces asymmetry in the coupling, and induces the counterbalancing lateral motion of a chimera state towards dynamically preferable centered position. The gain constants K_s and K_a govern the strength of the symmetric and the asymmetric parts of the control, respectively. In [59] we demonstrated the successful performance of the tweezer control scheme (1)–(6) in small nonlocally coupled networks of Van der Pol oscillators with $N = 48, 24, 12$. The characteristic signature of a chimera state is a pronounced difference of the average frequencies for oscillators belonging to the coherent and incoherent domain, respectively. The oscillators from the coherent domain are phase-locked and have equal frequencies, while the oscillators from the incoherent domain have different average frequencies which form typically an arc-like profile. We use the following definition of the mean phase velocities of the oscillators

$$\omega_k(t) = \frac{1}{\Delta T} \int_0^{\Delta T} \dot{\phi}_k(t-t') dt', \quad k = 1, \dots, N. \quad (7)$$

For the time window $\Delta T = 50$ Eq. (7) yields phase velocities averaged over $10^1 - 10^2$ oscillations. Plotting these functions $\omega_k(t)$ allows us to monitor the spatio-temporal phase dynamics of the system. On the other hand, using Eq. (7) with $t = \Delta T = 500000$ we obtain long-time averaged phase velocities, or average frequencies, which are denoted as $\langle \omega_k \rangle$.

When both the symmetric K_s and the asymmetric K_a control gains are switched on, the system develops a stable chimera state without any lateral motion of the coherent and incoherent domains. In the case when we switch off the asymmetric part of the control by fixing $K_a = 0$ and keep a positive symmetric gain $K_s > 0$, the chimera state starts to drift. This lateral motion becomes stronger for decreasing system size. To switch off both parts of the control, we replace σ_+ and σ_- with their effective time-averaged value $\langle \sigma \rangle = \frac{1}{2}[\langle \sigma_+ \rangle + \langle \sigma_- \rangle]$ where $\langle \sigma_+ \rangle$ and $\langle \sigma_- \rangle$ are time-averages of $\sigma_+(t)$ and $\sigma_-(t)$ obtained from the controlled reference case. In this case we observe a collapse of the chimera state.

Note that the tweezer control scheme is noninvasive on average only [57]. Indeed, for a non-invasively stabilized chimera state, the control terms σ_+ and σ_- must be time-independent. Moreover, one also must have $\sigma_+ = \sigma_-$. Figure 2(a) shows that this is not the case. Taking into account Eq. (6) and the definitions of Z_s and Z_a one easily sees that the instantaneous impact of tweezer control on the stabilized chimera state varies in time and can be strongly invasive. On the other hand, both terms $\sigma_+(t)$ and $\sigma_-(t)$ oscillate irregularly around almost the same constant level such that the time-average of Z_a vanishes and the time-average of $|Z_s|$ can be identified with the order parameter of the corresponding stabilized chimera state. Therefore, by analogy with [57] we can call our tweezer control scheme non-invasive on average.

The tweezer control scheme works effectively for fixed values of the control gains K_s and K_a . In order to obtain insight into the mechanism of the control scheme, and understand how to choose optimal values for control gains, we introduce the standard deviation of the mean phase velocity profile

$$\Delta_\omega = \sqrt{\frac{1}{N} \sum_{k=1}^N (\langle \omega_k \rangle - \Omega)^2}, \quad \text{where} \quad \Omega = \frac{1}{N} \sum_{k=1}^N \langle \omega_k \rangle. \quad (8)$$

Larger values of Δ_ω correspond to a well pronounced arc-like mean phase velocity profile, characterizing chimera states. Moreover, identifying the constant plateau in the graph of $\langle \omega_k \rangle$ we can find the

size of the chimera's coherent domain.

As an additional measure, we consider variations of the symmetric and asymmetric control inputs

$$\Delta Z_s = \max_t |Z_s| - \min_t |Z_s|, \quad \text{and} \quad \Delta Z_a = \max_t |Z_a|.$$

According to the tweezer control definition (6), products $K_s \Delta Z_s$ and $K_a \Delta Z_a$ characterize fluctuations of the control terms σ_{\pm} and of the difference $\sigma_+ - \sigma_-$, respectively. They can be used to measure the instantaneous invasiveness of the control scheme.

Figures 2(b),(c) show the dependence of $K_s \Delta Z_s$ on the symmetric control gain K_s (for fixed asymmetric gain $K_a = 2$), and the dependence of $K_a \Delta Z_a$ on the asymmetric control gain K_a (for fixed symmetric gain $K_s = 1$) in numerical simulations with $N = 24$ Van der Pol oscillators. The product $K_s \Delta Z_s$ vanishes for $K_s \rightarrow 0$ where control does not work and the system relaxes to the completely synchronized state. In the interval $K_s \in (0.5, 2)$ this product starts to grow slowly and we observe stabilization of chimera states. For $K_s > 2$ the tweezer control still stabilizes chimera states, but the product $K_s \Delta Z_s$ grows much faster. Comparing the behavior of $K_s \Delta Z_s$ with the behavior of the frequency variation Δ_{ω} and with the behavior of the coherent domain size for stabilized chimera states we note that the action of tweezer control is optimal for chimeras with large values of Δ_{ω} and with coherent domains comprising 10 – 40% of the system size.

Figure 2(c) shows that the instantaneous invasiveness of the asymmetric control $K_a \Delta Z_a$ grows almost linearly with increasing control gain K_a , therefore for optimal control design, the parameter K_a has to be as small as possible. However, it must not vanish completely, because otherwise the chimera state will start to move on the ring.

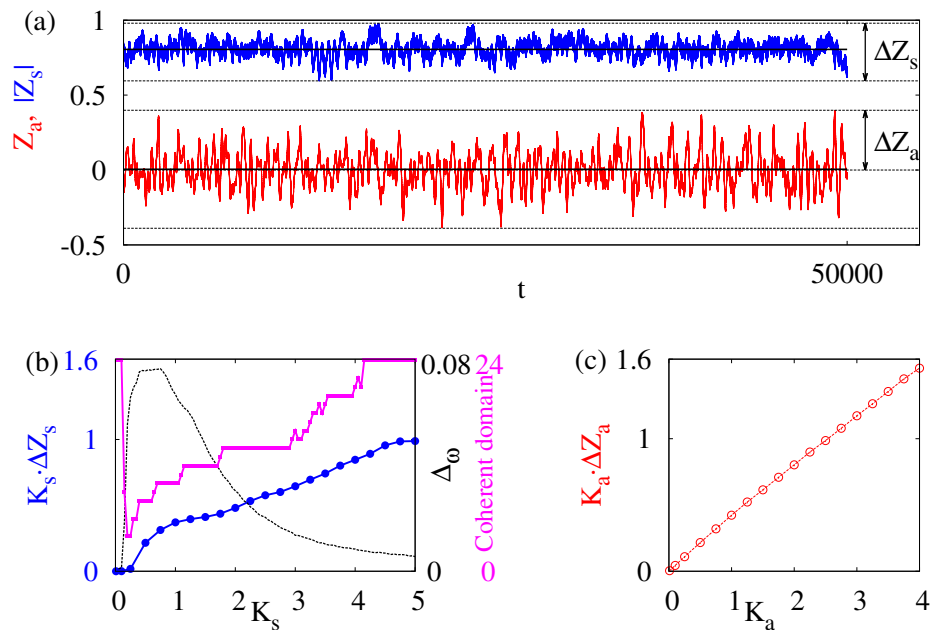


Figure 2: (a) Symmetric and asymmetric control inputs $|Z_s|$ (blue line) and Z_a (red line), respectively, for $N = 24$ Van der Pol oscillators, $R = 8$, $\varepsilon = 0.2$, $K_s = 1$, $K_a = 2$, after transient time $T = 500\,000$. Solid black lines denote time averaged values of Z_s and Z_a . (b), (c) Instantaneous invasiveness of symmetric control $K_s \Delta Z_s$ for $K_a = 2$ (b) and of asymmetric control $K_a \Delta Z_a$ for $K_s = 1$ (c) (lines with circles). The black (dashed) and purple (full) lines in panel (b) show the variance Δ_{ω} and the size of coherent domain for chimera states stabilized by tweezer control, respectively.

Using these preliminaries, we examine the influence of the control parameters K_s , K_a on the chimera behavior in networks of $N = 24$ Van der Pol oscillators, see Figure 3. Upper panels demonstrate the standard deviation of the mean phase velocity profiles for different types of local dynamics of the individual oscillators: $\varepsilon = 0.2$ (Fig 1(a))- sinusoidal limit cycle oscillations, $\varepsilon = 1$ (Fig 1(b)) and $\varepsilon = 5$ (Fig 1(c))- relaxation oscillations. Light colors correspond to larger values of standard deviation Δ_ω of the mean phase velocity profiles. Along the horizontal axis, for each ε there exists a range of parameter K_s , where the symmetric control is most efficient: for small values the symmetric control is not efficient, and for large K_s the chimera states approach the completely synchronized state ($\Delta_\omega = 0$). Larger values of ε result in an increasing amplitude of the limit cycle ($\varepsilon = 1, \varepsilon = 5$), and hence larger coupling strengths are required, therefore maximal values of Δ_ω are observed for larger K_s . Along the vertical axis, the standard deviation Δ_ω sharply increases for small values of the asymmetric control strength K_a , and then stays approximately at the same value indicating the saturation of the position control. Thus, choosing the control gain constants from this optimal light-colored region allows for stabilization of chimera states with the most pronounced mean phase velocity profiles. The diagrams were obtained numerically as an average over 100 realizations starting from random initial conditions and $\Delta T = 500000$.

The bottom panels, Fig. 3(d),(e),(f), depict the corresponding sizes of the coherent domains for chimera states with $\varepsilon = 0.2, 1, 5$, respectively. In our numerical experiments, the size of the coherent domain for a chimera state corresponds to the number of oscillators having equal mean phase velocities. In the parameter plane, we observe cascades of tongue-like regions depicting the increase of the size of the coherent domains with increasing symmetric control gain K_s . Comparing each pair of upper and lower panels in Fig. 3, we observe that the most pronounced difference between the values of mean phase velocity for the oscillators from the coherent and incoherent domain corresponds to chimera states with smallest coherent domains. Increasing the symmetric control gain results in decreasing difference, and at the same time increasing size of the coherent domain.

Note that the black regions in Fig. 3(a),(b),(c) and the yellow regions in Fig. 3(d),(e),(f), respectively,

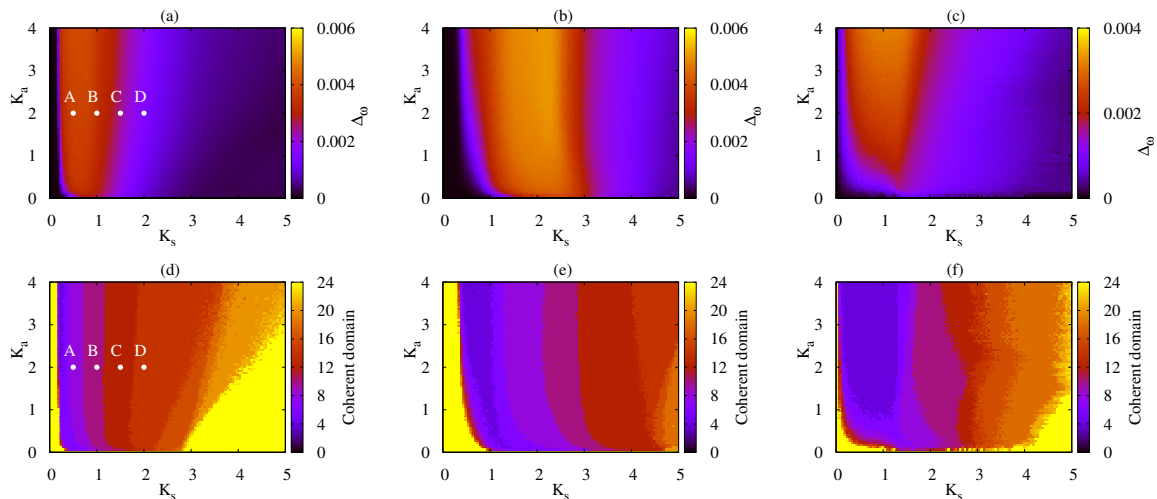


Figure 3: Control regimes of Van der Pol oscillator: Standard deviation Δ_ω of the mean phase velocity profiles for controlled chimera states in system Eqs. (1)-(6) in dependence on the control gains K_s , K_a for $N = 24$ oscillators, $R = 8$, $a = 0.02$, $\Delta T = 500\,000$: (a) $\varepsilon = 0.2$, (b) $\varepsilon = 1$, (c) $\varepsilon = 5$. Corresponding sizes of coherent domains for chimera states: (d) $\varepsilon = 0.2$, (e) $\varepsilon = 1$, (f) $\varepsilon = 5$. White dots A,B,C and D in panels (a),(d) correspond to the examples shown in Fig. 5.

have different meaning for the limits $K_s \rightarrow 0$ and $K_a \rightarrow 0$. This fact is illustrated in Figure 4 where we show the dependence of the time-averaged order parameter $\langle |Z_s| \rangle$ on the control gain K_s (for fixed $K_a = 2$) and on the control gain K_a (for fixed $K_s = 1$). If for $K_a > 0$ we switch off the symmetric control ($K_s = 0$), the system relaxes to the completely synchronized state with the global order parameter $|Z_s| = 1$, see Fig. 4(a). On the other hand, if for $K_s > 0$ we switch off the asymmetric control ($K_a = 0$), we obtain a dynamical state with global order parameter $|Z_s|$ close to that of the reference chimera state, see Fig. 4(b), but this state cannot be identified as a chimera because due to the fast wandering of its position we obtain $\langle \omega_1 \rangle = \langle \omega_2 \rangle = \dots = \langle \omega_N \rangle$. Actually, if we consider the interval $K_s \in [0.5, 2]$ with the most developed chimera states, i.e., chimeras with large values of $\Delta\omega$, then we find that the diagrams in Figure 3 show almost no dependence on K_a for $K_a \geq 2$. This allows us to identify tweezer control with $K_s \in [0.5, 2]$ and $K_a = 2$ as optimal.

White dots denoted as A,B,C,D in Fig. 3(a),(d) correspond to the examples shown in Fig. 5, which illustrate the dynamics of controlled system (1)–(6) of $N = 24$ coupled Van der Pol oscillators. To visualize the temporal dynamics of the oscillators we plot their mean phase velocities defined by (7) with $\Delta T = 50$. Panels (a)–(d) in Fig. 5 demonstrate that the size of the incoherent domain decreases.

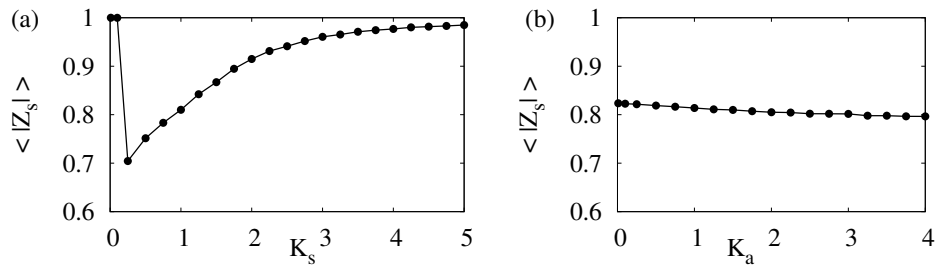


Figure 4: Time-averaged order parameter $\langle |Z_s| \rangle$ as a function of K_s (for fixed $K_a = 2$) and as a function of K_a (for fixed $K_s = 1$). Parameters: $N = 24$ Van der Pol oscillators, $R = 8$, $\varepsilon = 0.2$, $K_s = 1$, $K_a = 2$. Trajectory length $\Delta T = 500\,000$ and the same length of the discarded transient.

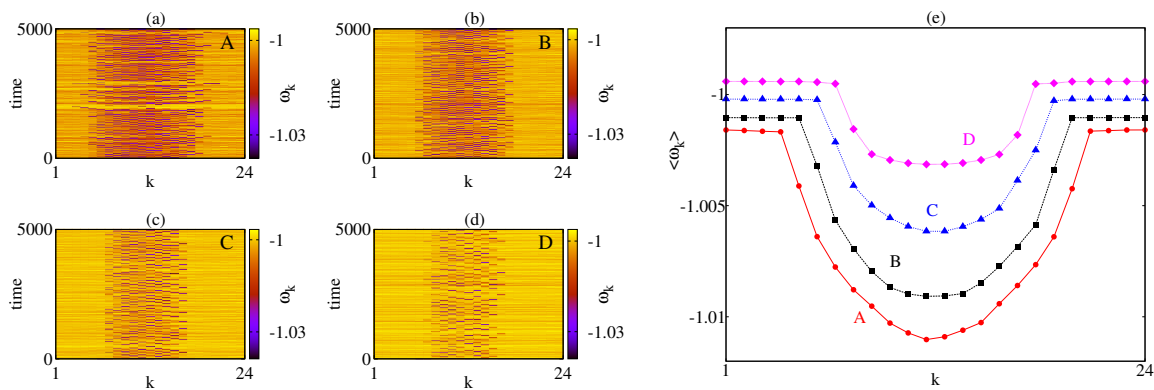


Figure 5: Mean phase velocities for a system of $N = 24$ Van der Pol oscillators, $R = 8$, $a = 0.02$, $\varepsilon = 0.2$ after a transient time of $T = 495\,000$: (a) $K_s = 0.5$, $K_a = 2$; (b) $K_s = 1$, $K_a = 2$; (c) $K_s = 1.5$, $K_a = 2$; (d) $K_s = 2$, $K_a = 2$. (e) Average frequency profiles corresponding to the chimera states shown in panels (a)–(d). Trajectory length $\Delta T = 500\,000$. Values of control gains K_s , K_a are denoted by white dots in Fig. 3(a),(d).

Fig. 5(e) shows phase velocity profiles for these four examples, averaged over $\Delta T = 500000$, where for example A ($K_s = 0.5$, $K_a = 2$) the chimera state is characterized by the largest difference of velocities for the coherent and incoherent oscillators, but at the same time has the smallest coherent domain consisting of 8 oscillators (red circles). Further increasing of K_s results in stabilization of chimera states with larger coherent domains.

To summarize, the tweezer control allows us not only to stabilize chimera states, but also to control the size of coherent and incoherent domains with appropriate choice of the control gains. Varying K_s and K_a , it is possible to solve different tasks: stabilize chimera states with maximal frequency difference for coherent and incoherent oscillators, or chimera states with largest coherent domain. The symmetric control gain K_s is crucial for the coherent domain size. The asymmetric control gain K_a usually exhibits saturation behavior, although for relaxation-type oscillations ($\varepsilon = 2$, $\varepsilon = 5$) larger values of K_a are optimal, while the amplitude of the limit cycle increases, and stronger coupling is needed for the synchronization.

3 Tweezer control in networks of FitzHugh-Nagumo oscillators

To emphasize the universality of the tweezer control scheme, we now consider FitzHugh-Nagumo oscillators:

$$\begin{aligned} \dot{X}_k = F_{\varepsilon,a}(X_k) &+ \frac{1}{R} \sum_{j=1}^R B_-(X_{k-j} - X_k) \\ &+ \frac{1}{R} \sum_{j=1}^R B_+(X_{k+j} - X_k), \end{aligned} \quad (9)$$

where $X_k = (u_k, v_k)^T \in \mathbb{R}^2$ is the state vector of the k -th oscillator and

$$F_{\varepsilon,a}(X_k) = \begin{pmatrix} (u_k - \frac{1}{3}u_k^3 - v_k)/\varepsilon \\ u_k + a \end{pmatrix} \quad (10)$$

is given by the nonlinear local dynamics of the FitzHugh-Nagumo model with time-scale parameter $\varepsilon > 0$, which we fix at $\varepsilon = 0.15$, and threshold parameter $a \in (-1, 1)$ in the oscillatory regime, i.e., each uncoupled oscillator exhibits a stable periodic orbit on a limit cycle. Again, we explore the nonlocal coupling topology, where each oscillator is coupled with R nearest neighbours to the left and right, and the matrices $B_-, B_+ \in \mathbb{R}^{2 \times 2}$ describe the coupling to the left and right, respectively.

System (9) with symmetric coupling

$$B_- = B_+ = bS(\psi),$$

where $b \in \mathbb{R}_+$ and

$$S(\psi) = \begin{pmatrix} \cos \psi & \sin \psi \\ -\sin \psi & \cos \psi \end{pmatrix} \quad (11)$$

is a rotational matrix with coupling phase ψ , has been considered in [17]. In this work, we have shown that chimera states can be observed for $\psi \lesssim \pi/2$, and we demonstrated that in the limit of small coupling strength $b \ll 1$ the phase dynamics of system (9) is approximately described by

$$\dot{\theta}_k = - \sum_{j=-R}^R \sin(\theta_k - \theta_{k+j} + \alpha)$$

where $\alpha \approx \psi$.

The tweezer control scheme for system (9) is introduced as

$$B_- = bS(\psi_-) \quad \text{and} \quad B_+ = bS(\psi_+) \quad (12)$$

where

$$\psi_{\pm} = \frac{\pi}{2} - K_s \left(1 - \frac{|Z_1 + Z_2|}{2} \right) \mp K_a (|Z_1| - |Z_2|), \quad (13)$$

with two complex order parameters

$$Z_1(t) = \frac{1}{[N/2]} \sum_{k=1}^{[N/2]} e^{i\xi_k(t)}$$

$$Z_2(t) = \frac{1}{[N/2]} \sum_{k=1}^{[N/2]} e^{i\xi_{N-k+1}(t)},$$

and $\xi_k(t)$ is the geometric phase of the k -th oscillator computed from

$$e^{i\xi_k(t)} = (u_k^2(t) + v_k^2(t))^{-1/2} (u_k(t) + iv_k(t)).$$

Similarly to the system of coupled Van der Pol oscillators, for an appropriate choice of control gains K_s and K_a in (13) we can stabilize chimera states in the system (9)-(13) with a small, as well as large, number of oscillators. To elaborate the issue of the optimal choice of the control gains, we will analyse the standard deviation of the mean phase velocity profile Δ_ω defined via the average frequencies $\langle \omega_k \rangle$ as in Eq. (8). Larger values of Δ_ω correspond to a well pronounced arc-like mean phase velocity profile, characterizing chimera states. Fig. 6(a),(b),(c) depicts values of Δ_ω in the plane of symmetric (K_s) and asymmetric (K_a) control gains for three values of the threshold parameter a of individual FitzHugh-Nagumo units (10), namely $a = 0.1$ (Fig. 6(a)), $a = 0.3$ (Fig. 6(b)), $a = 0.5$ (Fig. 6(c)). In all considered cases the individual FitzHugh-Nagumo oscillators are in the oscillatory regime, a change of parameter a results in the shift of one of the nullclines, and for larger values of parameter a the oscillator dynamics is more close to the bifurcation point ($a = 1$) on the transition from oscillatory to excitable regime. Light colours correspond to larger values of the standard deviation, which means well-pronounced mean phase velocity profile for obtained chimera state. The diagrams were obtained numerically as an average over 100 realizations starting from random initial conditions and integration time $\Delta T = 500000$.

For very small values of control gains, the control is not yet efficient (dark colour); with increasing K_s and K_a we obtain regions of optimal control (light colours) showing the maximal value of the standard deviation of the mean phase velocity profiles. In the system (9)-(13) we observe the qualitatively similar effect: the symmetric control gain K_s should be chosen within the optimal interval, while larger values push the system dynamics towards the synchronized state, the asymmetric control gain K_a shows the saturation behaviour, and its further increase does not affect strongly the dynamics of chimera states. The location of the optimal control gains depends on the threshold parameter a of the individual units. If we are far away from the bifurcation ($a = 0.1$ (Fig. 6(a))), then stronger coupling is required. With increasing a , the light optimal region moves to the left towards smaller values of symmetric control gain. The shape of the optimal (light colour) region does not change much, in contrast to the case of Van-der-Pol oscillators. This can be explained by the fact that a change of the threshold parameter a does not affect strongly the amplitude of the oscillators, while in the previous case the form of the limits cycle changes dramatically with the change of the parameter of individual oscillators.

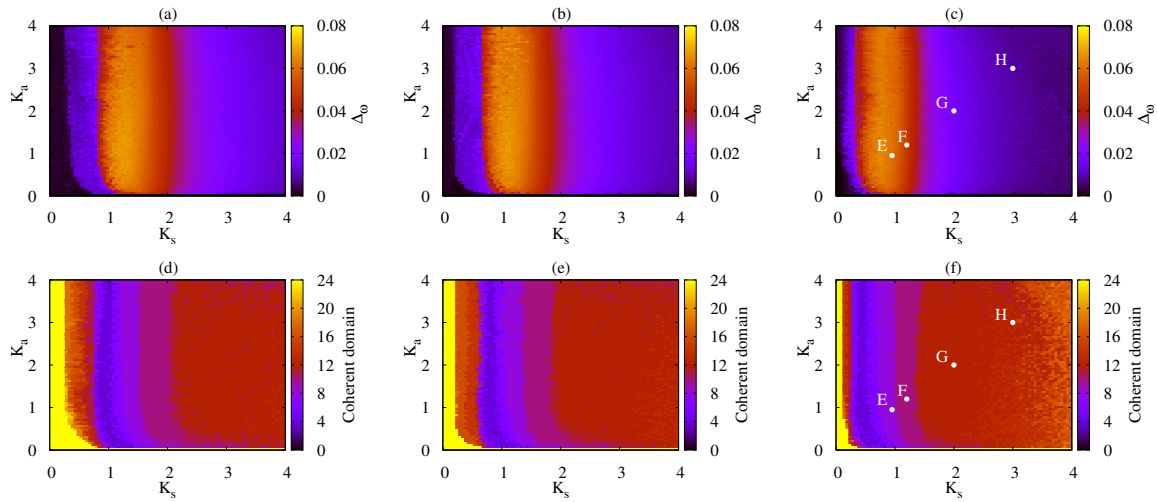


Figure 6: Control regimes of FitzHugh-Nagumo oscillator: Standard deviation Δ_ω of the mean phase velocity profiles for controlled chimera states in system Eqs. (9)-(13) depending on the control gains K_s , K_a for $N = 24$ oscillators, $R = 8$, $\varepsilon = 0.15$, $b = 0.15$, $\Delta T = 500\,000$: (a) $a = 0.1$, (b) $a = 0.3$, (c) $a = 0.5$ Corresponding sizes of coherent domains for chimera states: (d) $a = 0.1$, (e) $a = 0.3$, (f) $a = 0.5$. White dots E,F,G and H in panels (c),(f) correspond to the examples shown in Fig. 7.

The bottom panels Fig. 6(d),(e),(f) depict corresponding cascades of tongue-like regions for chimera states with different size of coherent domains. The most pronounced difference of the mean phase velocities for coherent and incoherent oscillators corresponds to chimera states with smallest coherent domains. Increasing the symmetric control gain causes stabilization of chimera states with larger coherent domains, but with smaller difference of frequencies. The location of these tongues shifts correspondingly towards smaller values with increasing threshold parameter a .

White dots denoted by E,F,G,H in Fig. 6(c),(f) show the fixed control gains values for the examples demonstrated in Fig. 7, which were obtained in the system of 24 FitzHugh-Nagumo oscillators with $R = 8$, and $a = 0.5$. First, we fix the control gains at the values $K_s = 1$ and $K_a = 1$ (point E in Fig. 6(c),(f)), the obtained chimera state is shown in Fig. 7(a) where we demonstrate the mean phase velocities for the system (9)-(13). Fig. 7(b) shows corresponding phase velocity profile averaged over time $\Delta T = 500\,000$ (top panel), snapshot of variables u_k at $t = 500\,000$ (middle panel), and snapshot in the (u_k, v_k) phase space (bottom panel). The chimera state has a large incoherent domain and well pronounced arc-like profile of averaged phase velocities. Increasing the control gains $K_s = 1.2$ and $K_a = 1.2$ (point F in Fig. 6(c),(f)) results in a chimera state with larger coherent domain, but smaller value of Δ_ω , shown in Fig. 7(c),(d). Note that the mean phase velocity profile shows a dip inside the incoherent domain. This phenomena has been first reported in [17] for a system of nonlocally coupled FitzHugh-Nagumo oscillators. There we have shown that stronger coupling causes the transition to chimera states with multiple incoherent domains, evolving from one large incoherent domain. Increasing of the coupling strength causes appearance of one or more dips in the mean velocity profiles, which finally gives birth to multichimera states. This phenomena was possible to observe in large networks, like 1000 coupled oscillators.

In our system (9)-(13), the tweezer control enables the observation of multichimera states in small systems, which was not possible before. Fig. 7(e),(f) demonstrates stabilized chimera states with two incoherent domains for $K_s = 2$ and $K_a = 2$ (point G in Fig. 6(c),(f)), and Fig. 7(g),(h) shows chimera states with three incoherent domains for $K_s = 3$ and $K_a = 3$ (point H in Fig. 6(c),(f)), which appear for

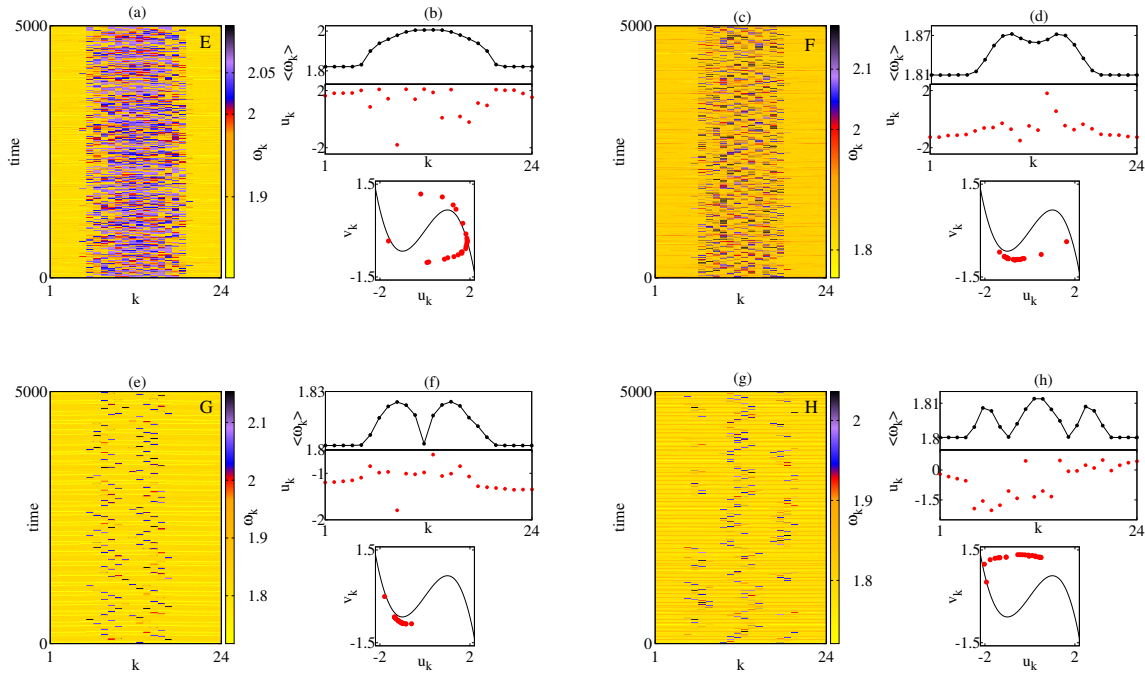


Figure 7: (a) Mean phase velocities for a system of $N = 24$ FitzHugh-Nagumo oscillators, and $R = 8$, $\varepsilon = 0.15$, $b = 0.15$, $a = 0.5$, after a transient time $T = 495000$; (b) phase velocity profile averaged over $\Delta T = 500000$ (top panel), snapshot of variables u_k (middle panel), and snapshot in the (u_k, v_k) phase space at time $t = 500000$ (bottom panel, cubic nullcline of the uncoupled FitzHugh-Nagumo unit shown in black), control gains $K_s = 1$, $K_a = 1$, denoted by point E in Fig. 6(c),(f). Same for other values of control gains: (c),(d) $K_s = 1.2$, $K_a = 1.2$; (e),(f) $K_s = 2$, $K_a = 2$; (g),(h) $K_s = 3$, $K_a = 3$, denoted by F, G, H correspondingly in Fig. 6(c),(f).

increasing values of both control gains. Their coherent domains, including small domains in between the incoherent ones, have large size, at the same time the difference between averaged frequencies for coherent and incoherent oscillators decreases.

In the considered networks of FitzHugh-Nagumo oscillators, the tweezer control scheme works efficiently, stabilizing chimera states. Moreover, it enables the observation of multichimera states in a system of small size.

4 Conclusion

Tweezer control allows for effective stabilization of chimera states in large and in small-size networks of nonlinear oscillators. It is a combination of two instruments, the symmetric control term suppresses the chimera collapse, and the asymmetric control stabilizes the spatial position of a chimera state. We have provided an extensive numerical analysis of the parameter space of the control gains in order to find the regions for the most effective stabilization of chimera states in the nonlocally coupled networks of Van der Pol and FitzHugh-Nagumo oscillators. As a criterion for chimera patterns we have used the standard deviation of the mean phase velocity profiles, and the size of the coherent domains.

The dynamics of the individual oscillators influences the shape of the controlled chimera states. In networks of Van der Pol oscillators with sinusoidal individual oscillations (small parameter ε) for the

effective stabilization of chimera states the symmetric control gain K_s has to be fixed at intermediate values $K_s \in (0.3, 2)$, and the asymmetric control gain K_a has weaker influence, it must be chosen at least larger than $K_a = 0.1$. Further increasing the asymmetric control does not affect strongly the stabilized chimera states. If individual Van der Pol oscillations perform relaxation oscillations (large parameter ε), the symmetric control gain must be chosen larger, approximately $K_s \in (1, 3)$, the asymmetric control gain K_a now has a stronger influence on the chimera shape and must be larger as well, due to the increased amplitude of the individual limit cycle. The symmetric control gain K_s is essential for the size of the coherent domain in the stabilized chimera states, larger values promote increasing size of the coherent domain.

Finally, with appropriate choice of control gains either the chimera state with the most pronounced frequency difference (but smaller coherent domain) can be stabilized, or the chimera state with larger coherent domain but less pronounced frequency difference.

In networks of FitzHugh-Nagumo oscillators, a change of the threshold parameter a results in a slight shift of the optimal control region in the parameter plane, while the amplitude of the individual limit cycle is unchanged. As in the previous case, the symmetric control gain K_s is more essential, and when chosen optimally, the asymmetric control gain can be again relatively small. The interesting aspect is that tweezer control allows for the stabilization of chimera states with multiple incoherent domains in small-size networks.

Our results can be useful for the experimental realizations of chimera states in small networks, since the optimal choice of the symmetric and asymmetric control gains can facilitate the observation of preferable chimera patterns.

References

- [1] Y. Kuramoto and D. Battogtokh, *Nonlin. Phen. in Complex Sys.* **5**, 380 (2002).
- [2] D. M. Abrams and S. H. Strogatz, *Phys. Rev. Lett.* **93**, 174102 (2004).
- [3] S.-I. Shima and Y. Kuramoto, *Phys. Rev. E* **69**, 036213 (2004).
- [4] C. R. Laing, *Physica D* **238**, 1569 (2009).
- [5] A. E. Motter, *Nature Physics* **6**, 164 (2010).
- [6] M. J. Panaggio and D. M. Abrams, *Nonlinearity* **28**, R67 (2015).
- [7] E. Schöll, *Eur. Phys. J. Spec. Top.* **225**, 891 (2016).
- [8] H. Sakaguchi, *Phys. Rev. E* **73**, 031907 (2006).
- [9] G. C. Sethia, A. Sen, and F. M. Atay, *Phys. Rev. Lett.* **100**, 144102 (2008).
- [10] E. A. Martens, C. R. Laing, and S. H. Strogatz, *Phys. Rev. Lett.* **104**, 044101 (2010).
- [11] E. A. Martens, *Chaos* **20**, 043122 (2010).
- [12] I. Omelchenko, Y. L. Maistrenko, P. Hövel, and E. Schöll, *Phys. Rev. Lett.* **106**, 234102 (2011).
- [13] M. Wolfrum, O. E. Omel'chenko, S. Yanchuk, and Y. L. Maistrenko, *Chaos* **21**, 013112 (2011).

- [14] M. Wolfrum and O. E. Omel'chenko, *Phys. Rev. E* **84**, 015201 (2011).
- [15] O. E. Omel'chenko, M. Wolfrum, S. Yanchuk, Y. L. Maistrenko, and O. Sudakov, *Phys. Rev. E* **85**, 036210 (2012).
- [16] I. Omelchenko, B. Riemenschneider, P. Hövel, Y. L. Maistrenko, and E. Schöll, *Phys. Rev. E* **85**, 026212 (2012).
- [17] I. Omelchenko, O. E. Omel'chenko, P. Hövel, and E. Schöll, *Phys. Rev. Lett.* **110**, 224101 (2013).
- [18] M. J. Panaggio and D. M. Abrams, *Phys. Rev. Lett.* **110**, 094102 (2013).
- [19] G. C. Sethia, A. Sen, and G. L. Johnston, *Phys. Rev. E* **88**, 042917 (2013).
- [20] G. C. Sethia and A. Sen, *Phys. Rev. Lett.* **112**, 144101 (2014).
- [21] J. Hizanidis, V. Kanas, A. Bezerianos, and T. Bountis, *Int. J. Bif. Chaos* **24**, 1450030 (2014).
- [22] A. Zakharova, M. Kapeller, and E. Schöll, *Phys. Rev. Lett.* **112**, 154101 (2014).
- [23] A. Yeldesbay, A. Pikovsky, and M. Rosenblum, *Phys. Rev. Lett.* **112**, 144103 (2014).
- [24] J. Xie, E. Knobloch, and H.-C. Kao, *Phys. Rev. E* **90**, 022919 (2014).
- [25] C. R. Laing, *Phys. Rev. E* **90**, 010901 (2014).
- [26] Yu. Maistrenko, A. Vasylenko, O. Sudakov, R. Levchenko, V. Maistrenko, *Int. J. Bif. Chaos* **24** (8), 1440014 (2014).
- [27] Yu. Maistrenko, O. Sudakov, O. Osiv, and V. Maistrenko, *New. J. Phys.* **17**, 073037 (2015).
- [28] L. Schmidt and K. Krischer, *Phys. Rev. Lett.* **114**, 034101 (2015).
- [29] M. Wolfrum, O. E. Omel'chenko, and J. Sieber, *Chaos* **25**, 053113 (2015).
- [30] I. Omelchenko, A. Provata, J. Hizanidis, E. Schöll, and P. Hövel, *Phys. Rev. E* **91**, 022917 (2015).
- [31] M. J. Panaggio and D. M. Abrams, *Phys. Rev. E* **91**, 022909 (2015).
- [32] C. R. Laing, *Phys. Rev. E* **92**, 050904(R) (2015).
- [33] S. Olmi, E. A. Martens, S. Thutupalli, and A. Torcini, *Phys. Rev. E* **92**, 030901(R) (2015).
- [34] J. Hizanidis, E. Panagakou, I. Omelchenko, E. Schöll, P. Hövel, and A. Provata, *Phys. Rev. E* **92**, 012915 (2015).
- [35] I. Omelchenko, A. Zakharova, P. Hövel, J. Siebert, and E. Schöll, *Chaos* **25**, 083104 (2015).
- [36] A. Hagerstrom, T. E. Murphy, R. Roy, P. Hövel, I. Omelchenko, and E. Schöll, *Nature Physics* **8**, 658 (2012).
- [37] M. R. Tinsley, S. Nkomo, and K. Showalter, *Nature Physics* **8**, 662 (2012).
- [38] S. Nkomo, M. R. Tinsley, K. Showalter, *Phys. Rev. Lett.* **110**, 244102 (2013).
- [39] E. A. Martens, S. Thutupalli, A. Fourrière, and O. Hallatschek, *Proc. Nat. Acad. Sciences* **110**, 10563 (2013).

- [40] L. Larger, B. Penkovsky, and Y. L. Maistrenko, *Phys. Rev. Lett.* **111**, 054103 (2013).
- [41] L. Larger, B. Penkovsky, and Y. Maistrenko, *Nature Comm.* **6**, 7752 (2015).
- [42] L. V. Gambuzza, A. Buscarino, S. Chessari, L. Fortuna, R. Meucci, and M. Frasca, *Phys. Rev. E* **90**, 032905 (2014).
- [43] M. Wickramasinghe and I. Z. Kiss, *PLoS ONE* **8**, e80586 (2013).
- [44] L. Schmidt, K. Schönleber, K. Krischer, and V. Garcia-Morales, *Chaos* **24**, 013102 (2014).
- [45] D. P. Rosin, D. Rontani, N. D. Haynes, E. Schöll, and D. J. Gauthier, *Phys. Rev. E* **90**, 030902(R) (2014).
- [46] E. Ott and T. M. Antonsen, *Chaos* **18** 037113 (2008).
- [47] E. Ott and T. M. Antonsen, *Chaos* **19** 023117 (2009).
- [48] O. E. Omel'chenko, *Nonlinearity* **26**, 2469 (2013).
- [49] D. Pazó and E. Montbrió, *Phys. Rev. X* **4**, 011009 (2014).
- [50] P. Ashwin, and O. Burylko, *Chaos* **25**, 013106 (2015).
- [51] M. J. Panaggio, D. M. Abrams, P. Ashwin, and C. R. Laing, *Phys. Rev. E* **93**, 012218 (2016).
- [52] F. Böhm, A. Zakharova, E. Schöll, and K. Lüdge, *Phys. Rev. E* **91**, 040901(R) (2015).
- [53] J. D. Hart, K. Bansal, T. E. Murphy, and R. Roy, *Chaos* **26**, 094801 (2016).
- [54] O. E. Omel'chenko, M. Wolfrum, and Yu. L. Maistrenko, *Phys. Rev. E* **81**, 065201 (2010).
- [55] Y. Suda and K. Okuda, *Phys. Rev. E* **92**, 060901(R) (2015).
- [56] C. Bick, M. Sebek, and I. Z. Kiss, *arXiv:1705.05812* (2017).
- [57] J. Sieber, O. E. Omel'chenko, and M. Wolfrum, *Phys. Rev. Lett.* **112**, 054102 (2014).
- [58] C. Bick and E. Martens, *New J. Phys.* **17**, 033030 (2015).
- [59] I. Omelchenko, O. E. Omel'chenko, A. Zakharova, M. Wolfrum, and E. Schöll, *Phys. Rev. Lett.* **116**, 114101 (2016).